RESEARCH ARTICLE
doi: 10.2306/scienceasia1513-1874.2015.41.055

ScienceAsia 41 (2015): **55–63**

Evidence of Holocene sea level regression from Chumphon coast of the Gulf of Thailand

Parisa Nimnate[a], **Vichai Chutakositkanon**[a,*], **Montri Choowong**[a,b], **Santi Pailoplee**[a,b], **Sumet Phantuwongraj**[a]

[a] Department of Geology, Faculty of Science, Chulalongkorn University, Bangkok 10330 Thailand
[b] Earthquake and Tectonic Geology Research Unit (EATGRU), Department of Geology, Faculty of Science, Chulalongkorn University, Bangkok 10330 Thailand

*Corresponding author, e-mail: vichai.c@yahoo.com

Received 15 Oct 2014
Accepted 1 Dec 2014

ABSTRACT: Sets of beach ridge plains located as far as ten kilometres inland at the Chumphon estuary area, southern peninsular Thailand, provide evidence of an ancient sea-level change. Relict coastal landforms including former beach ridge plains, old lagoons, swales, and former tidal flats between beach ridges are found inland at elevations of 1–5 m above the present sea level. Ancient beach ridges here comprise three sets and all are inferred to have been deposited during the Holocene. The orientation of the inner beach ridge plains confirms their deposition by south to north longshore currents, whereas the middle and outer ridges were probably formed by north-to-south currents. Grain size analysis shows that all ancient beach ridge deposits are similar and are composed of fine- to medium-grained sand with high sphericity. Likewise, the compositions are similar, with quartz as a major component and feldspar and ferromagnesian minerals as minor components, reflecting the same sediment provenance. Marine fossils found in the former tidal deposit indicate intertidal and mangrove environments. Optical stimulating luminescence dating of three sets of beach ridge plains indicate that deposition occurred 8900–5600, 5900–2700, and 3800–1600 years ago for inner, middle, and outer beach ridge plains, respectively.

KEYWORDS: beach ridge plain, progradation, sea level curve, palaeo-shoreline, Pleistocene

INTRODUCTION

Since 1980, sea level changes in Thailand have been extensively investigated on the lower central plain and Holocene palaeo-shorelines proposed[1–10]. The Holocene sea level curve for peninsular Malaysia and Singapore were among the first pioneer curves that derived from result of radiocarbon dating of shell, wood, and coral materials in marine and brackish deposits[11,12]. Most of the dated material comes from estuarine environment and indicates the history of sea level change during the Holocene after the post-glacial marine transgression (PGMT). In general, the sea level rose rapidly after PGMT from several meters below the present mean sea level (MSL) and reached a highstand of nearly 4 m above MSL at around 6500–7000 years before present (BP). Then sea level began to fall to the present MSL around 3000 or fewer years ago[11,13]. From southern Thailand, Sconffin and Tissier also confirmed this history of sea level changes from a study of fringing reefs growing in the muddy waters of southeast Phuket[14]. The results indicated that reefs commenced to grow 6000 years ago when the sea level (low spring tide) was at 1 m above present MSL[14]. Moving northwards to the upper Gulf of Thailand, an indicator of Holocene marine transgression is found in the lower central plain from the deposition of the Bangkok clay formation[15]. However, fluctuations of sea level were also reported locally from Thailand and peninsular Malaysia during sea-level regression after the sea reached the mid-Holocene highstand[12,16]. A sea-level curve in the Gulf was firstly established by Sinsakul[16]. Radiocarbon dating suggest that sea level rose rapidly from −12.75 m below MSL to reach a maximum highstand at about 3.5 m above present MSL at around 6500 to 4000 years ago[17,18].

Well accepted evidence of sea level changes is provided by muddy deposition especially from marine and brackish fossils. Relict of coastal landforms preserved inland are significant evidence rarely discovered. In this study, we focus on our discovery on the Chumphon estuary area, southern Thailand where the relict beach ridge plains remain as far as ten kilometres inland. The estuary area of

Chumphon preserves spectacular geomorphological landforms as the former beach ridges 6–10 km from the present shoreline. These beach ridge plains are geographically bordered by the highland in the west and the present coastline in the east (Fig. 1). In the middle part of the area, the Thatapaow canal runs throughout Muang district and flow down south to reach the coastal zone joining Sawi and Langsuan rivers at Sawi and Langsuan districts, respectively. Terrestrial sediments are transported to the Chumphon coastal zone via all these rivers.

MATERIALS AND METHODS

Geomorphological interpretation and field planning

Relict landforms including three different beach ridge plains can be recognized clearly from aerial photographs taken in 1998 by the Royal Thai Survey Department (Fig. 1a). Detail interpretation from aerial photographs provides a coastal geomorphological map with a precise boundary classification of landforms. The interpretation of palaeo-longshore current is also provided by the orientation of beach ridges. The coastal transect lines were then set up mostly perpendicular to the present shoreline for geomorphological checking and locating sampling sites. Geomorphological field check is not only aimed to examine the accuracy of interpretation, but also to make a detail topographical survey of beach ridge plains by high accuracy digital GPS. Samples for detailed analysis of sedimentary deposits from each beach ridge were collected by digging small excavation pit as well as hand augering. Apart from beach ridges, sediment samples were also taken from several landforms including a former lagoon, former tidal flat, and modern beach. At the top of each beach ridge, shallow pits were done at foreshore zone and sand samples were collected for optically stimulated luminescence (OSL) dating. Marine and brackish shell fossils were also collected from former tidal flats and swales for systematic faunal classification (also see location in Fig. 1b).

Laboratory analysis

A total of 115 samples from 22 auger cores of the former sandy beach ridges, and the recent beach were analysed. Distribution of grain size and the statistical values of sediments were calculated by moment method modified from Boggs[19] and four parameters were determined: average grain size, standard deviation, skewness, and kurtosis. The comparison of moment parameter followed Blott

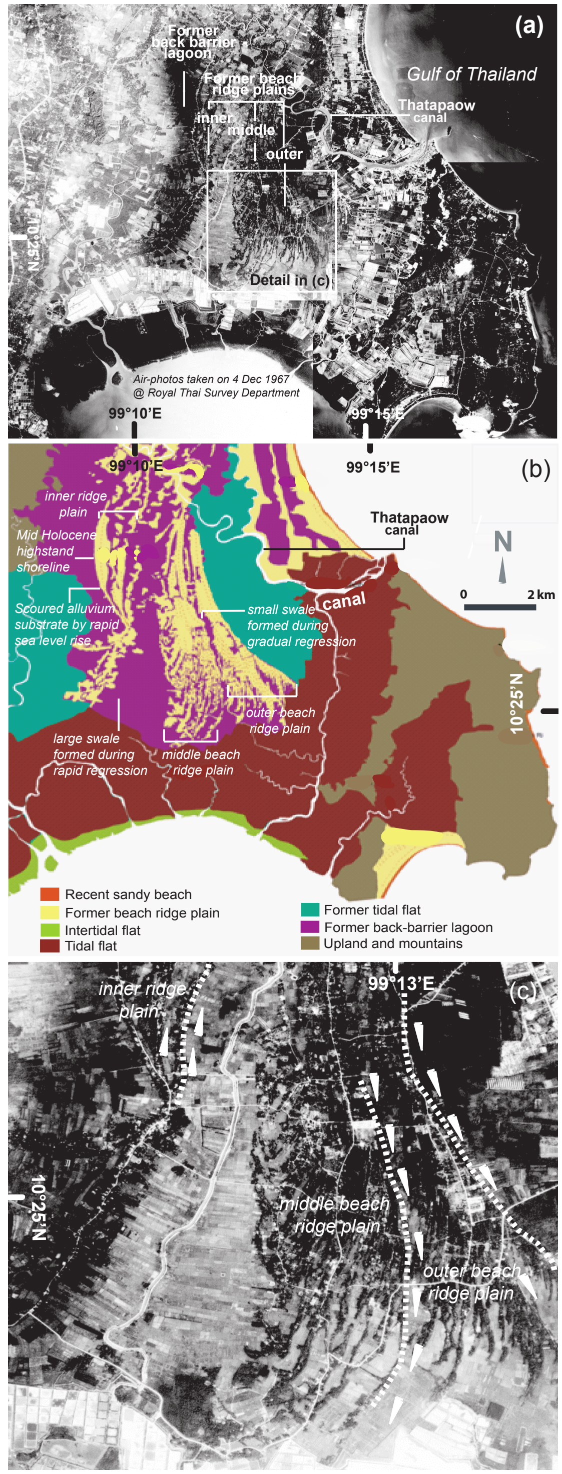

Fig. 1 (a) Aerial photographs with approximately 1:50 000 scale covering the study area (modified from Thai Royal survey Department, 1998). (b) Coastal geomorphological map displays all important landforms. (c) Close-up beach ridge plains with interpreted palaeo-longshore currents (arrows).

and Pye[20]. Sediment was classified by binocular microscope. The percentage was estimated by comparison with the standard chart of sediment composition[21]. The classification of roundness and sphericity followed Powers[22].

RESULTS

Description of landforms

The result of aerial photograph interpretation (Fig. 1a) provides a detailed geomorphological map (Fig. 1b). Coastal geomorphological units observed in this area include the old sandy beach, old lagoon, young sandy beach, old tidal flat, upland and mountain, intertidal flat, and tidal flat. Some relict coastal landforms were recognized inland as far as ten kilometres from the present shoreline, e.g., a series of ancient beach ridges. Inland beach ridges showing a strandline can be used as an indicator of the palaeo-shoreline. The former beach ridge is a relict feature left behind inland usually of interest for being evidence of sea level changes both during marine transgression and regression. Likewise, sets of strandlines indicate the past longshore current direction. The shape of the ancient beach ridge can also be related to the sea level regression at the time when the land prograded seawards. In this area, at least three series of former beach ridges were recognized with a different direction of palaeo-longshore current. The inner series showed the direction of palaeo-longshore current from the south to the north. On the other hand, the middle and outer series of former beach ridges showed the palaeo-longshore current direction from the north to the south (Fig. 1c).

Physical properties of the sediments

Plotting of statistical parameters from grain size analysis (Fig. 2) can separate the sediments into four groups based on the different landforms as inner series, middle series, outer series, and recent beach. Mean grain size of the inner series of former beach ridge is characterized as very fine to medium sand, moderately to moderately well sorted. Skewness and kurtosis values are showed as coarse to fine skewed to very leptokurtic, respectively. From the middle series, mean grain size is described as medium sand and moderately sorted. Skewness value showed as symmetrical to fine skewed, whereas kurtosis value is in the range of very leptokurtic. Mean grain size of the outer series of former beach ridges is classified as fine sand, moderately to moderately well sorted, coarse

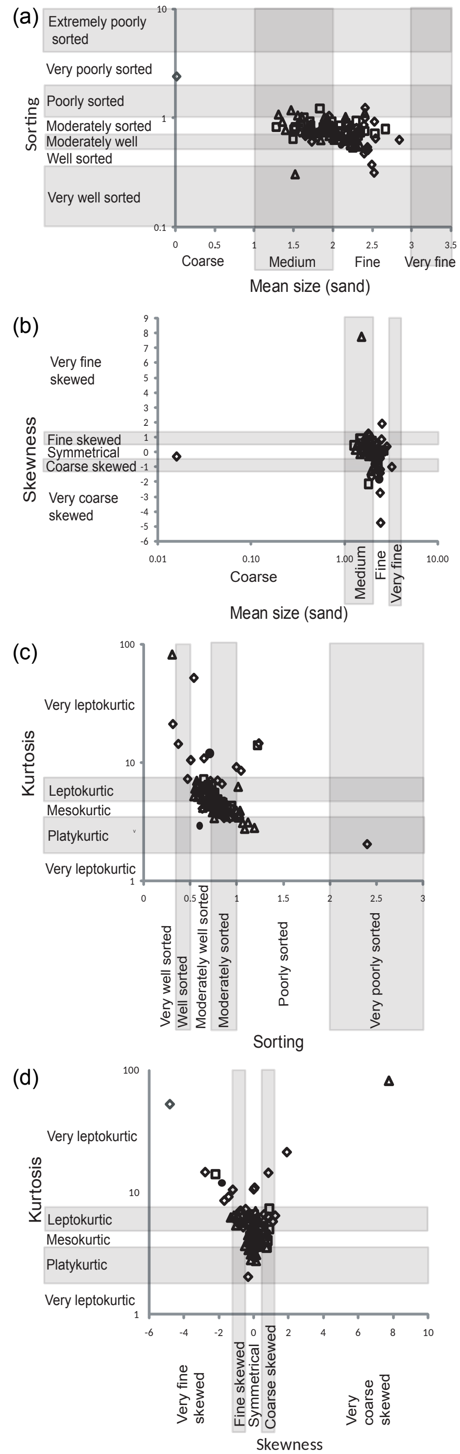

Fig. 2 Scatter plots of statistic parameter relationships: (a) mean size versus sorting, (b) mean size versus skewness, (c) sorting versus kurtosis, and (d) skewness versus kurtosis. Diamonds: inner ridge, squares: middle ridge, triangles: outer ridge, and circles: recent beach.

to symmetrical skewed, with a kurtosis value is in the range of very mesokurtic to leptokurtic. The recent beach is dominated by fine sand, moderately to moderately well sorted, symmetrical skewed, and leptokurtic.

Two-variable scatter plots include mean grain size versus sorting, mean grain size versus skewness, sorting versus kurtosis, and skewness versus kurtosis[23]. Mean grain size versus sorting (i.e., standard deviation) (Fig. 2a) is commonly used to indicate the deposition environment of the sediment sample. The middle, outer ridge, and recent beach sand samples had a mean grain size between medium sand and fine sand. Sorting value was in a range of moderately to moderately well sorted. Mean grain size versus skewness in this unimodal sediment is composed of pure sand and shown positive skewed. Scatter plot of mean grain size versus standard deviation are shown in Fig. 2b. Some sand sediments at the outer ridge and the inner ridge showed extreme kurtosis values and good sorting (Fig. 2c) similar to sediments in the neritic zone. Extreme kurtosis values result from sand mode that achieves a good sorting in a high energy environment of a beach, and then it is transported a mass by storm to a neritic environment where it becomes mixed with clay and hence is finally deposited in a medium of low sorting efficiency[23].

Skewness versus kurtosis (Fig. 2d)[24] shows a regular path. Most of the samples are in the range of fine to coarse skewed and mesokurtic to leptokurtic. Half of all sediment samples are characteristically leptokurtic and positive skewed, indicating that they have been transported not far from the sort area.

Compositions, roundness, and sphericity

The old beach ridge at Chumphon estuary area consists mainly of quartz. All beach ridges, the inner, the middle, and the outer series of old beach contain similar composition. A minor component of the inner series of old beach consist of feldspar and ferromagnesian minerals, in a percentage higher than that of the middle and the outer ridge (Fig. 3).

Roundness of the inner beach sediments displays a subangular shape, whereas, the middle beach ridge shows an angular to subangular shape. Roundness trend from the outer former beach ridge is subangular. All of beach ridge sediments show a high sphericity shape.

Based on the composition of beach sediments, sediments in this coastal area were transported from mountains in the west and the north of this area. Rock basements are composed of Permo-carboniferous and Permian sedimentary rocks. The weathered sediments from these rock basements were transported by active fluvial systems in the north-eastern part of beach ridges and through the coastal zone by longshore currents[25].

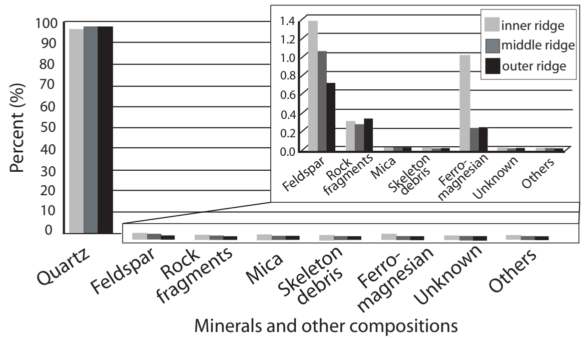

Fig. 3 Histogram of sediment composition from three sets of beach ridge plains (see text for explanation).

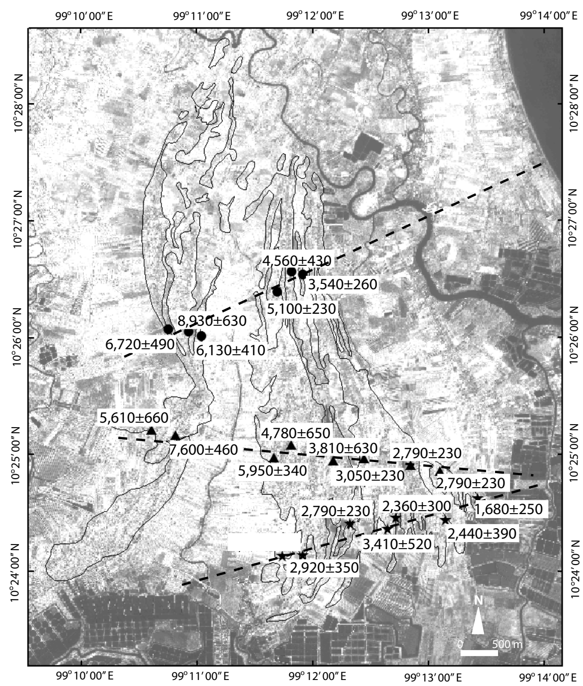

Fig. 4 Locations and results of OSL dating along three transects. Black circles indicate pit locations along transect 1, black triangles belong to transect 2, and black stars represent locations of pit along transect 3. Dark lines indicate tentative boundary of beach ridges.

Age determination of ancient beach ridges

Twenty one samples from the ancient beach ridge plains (Figs. 4 and 5a) located far from present

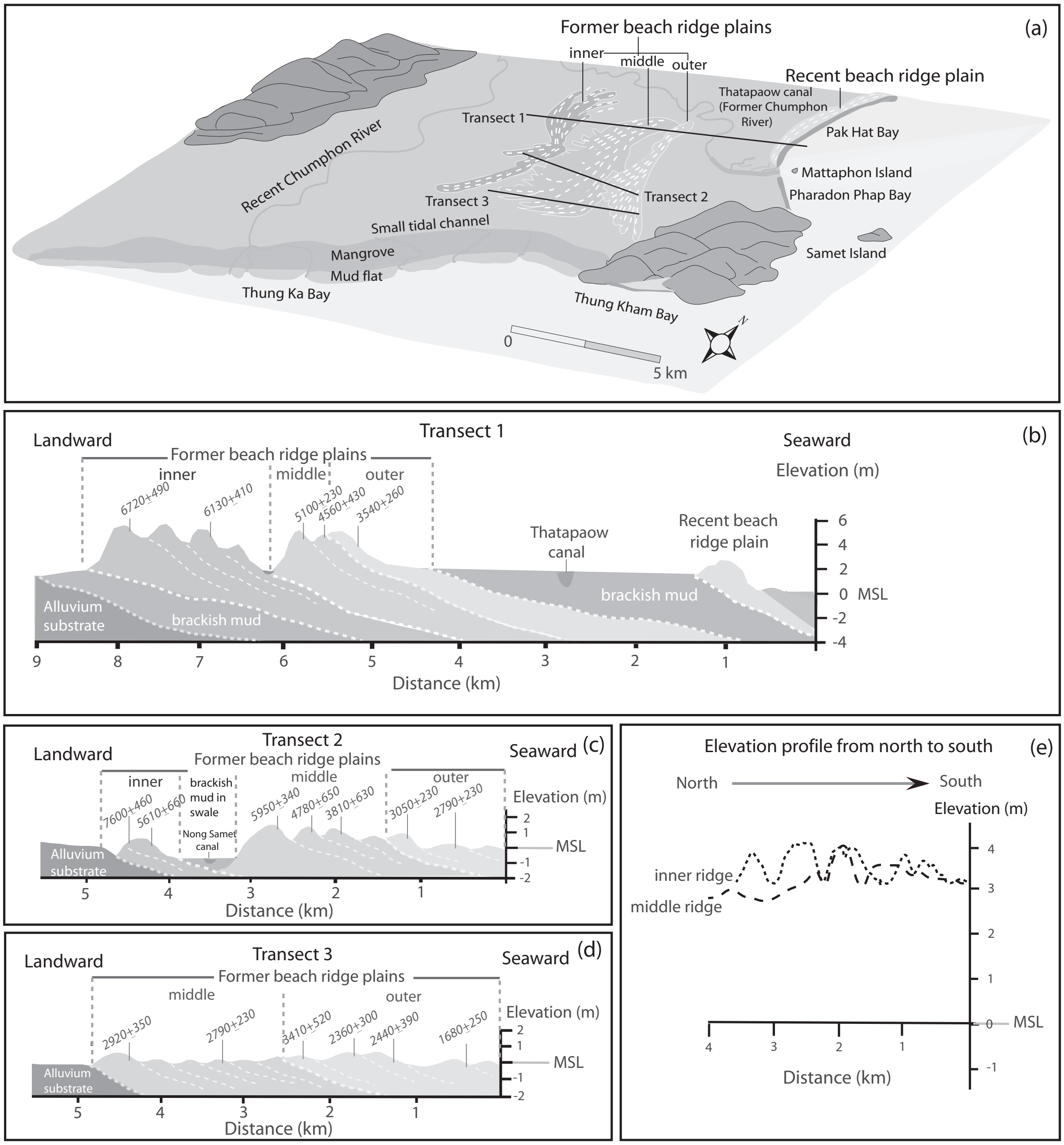

Fig. 5 Three dimension geographical models and cross-sections with age determination. Numbers in (b) and (c) indicate the age determined by OSL dating (see text for explanation).

shoreline were analysed by the optical stimulate luminescence (OSL) dating method. The age of these beach ridges dated from all transects is shown in Table 1 and Fig. 5b–d.

At transect 1, result of OSL dating of the inner ridge series reveals an age of between 8930 ± 630–6130 ± 410 years BP. The middle beach ridges series have an age of between 5100 ± 230–4560 ± 430 years BP. Finally, the outer ridge series have a younger age than those of inner and middle ridge plains around 3540 ± 260 years BP.

Along transect 2, OSL samples were collected from 8 locations at the inner, middle, and outer beach ridge series. The age of beach sand at the inner beach ridges ranges from 7600 ± 460–5610 ± 600 years BP. Whereas, the middle ridge shown the age of deposition from 5950 ± 340, 4780 ± 650 and 3180 ± 630 years BP seawards. The

Table 1 Result of OSL dating of the beach ridges from Chumphon area, southern Thailand (see locations of sample collection in Figs. 4 and 5a–c).

Transect	Latitude (° N)	Longitude (° E)	$Dist_s$ (km)	Depth (m)	K (%)	U (ppm)	Th (ppm)	Moist. (%)	Dose rate (mGy/a)	D_e (mGy)	Age (years)
Line 1											
1–1	10.434595	99.179238	6.49	0.15	0.156	3.70	16.0	10.2	2.53 ± 0.25	17.0 ± 1.0	6720 ± 490
1–2	10.434304	99.182170	6.30	0.55	0.377	1.27	4.94	3.72	1.58 ± 0.15	21.0 ± 1.9	8930 ± 630
1–3	10.433588	99.184089	6.10	0.60	0.155	2.69	13.3	2.04	2.08 ± 0.20	12.0 ± 0.6	6130 ± 410
1–4	10.439976	99.195011	4.75	0.65	0.449	1.64	7.14	6.59	1.98 ± 0.19	10.0 ± 0.5	5100 ± 230
1–5	10.442778	99.196986	4.33	0.55	0.517	1.09	2.86	2.62	1.68 ± 0.16	7.6 ± 1.4	4560 ± 430
1–6	10.442361	99.198686	4.20	0.45	0.402	2.23	13.6	2.62	2.51 ± 0.25	8.8 ± 0.5	3540 ± 260
Line 2											
2–1	10.415228	99.214072	7.54	0.45	0.317	6.34	34.9	8.69	4.93 ± 0.49	13.0 ± 0.1	5610 ± 660
2–2	10.414320	99.218274	7.29	0.22	0.224	1.88	4.67	3.72	1.38 ± 0.13	22.0 ± 1.0	7600 ± 460
2–3	10.420207	99.176836	6.53	0.35	0.372	2.68	8.84	2.34	2.20 ± 0.22	18.0 ± 0.8	5950 ± 340
2–4	10.419499	99.180280	6.00	0.43	0.479	1.35	4.96	7.06	1.82 ± 0.18	13.0 ± 0.5	4780 ± 650
2–5	10.416280	99.194412	5.67	0.24	0.448	1.66	7.23	5.12	1.99 ± 0.19	5.9 ± 0.9	3810 ± 630
2–6	10.418078	99.196943	5.60	0.37	0.414	1.02	5.33	2.68	1.62 ± 0.16	4.7 ± 0.2	3050 ± 230
2–7	10.415877	99.202926	5.00	0.23	0.345	1.31	5.32	3.36	1.55 ± 0.15	5.3 ± 0.5	2790 ± 230
2–8	10.416145	99.207339	4.68	0.30	0.229	2.31	10.7	7.15	1.95 ± 0.19	5.3 ± 0.5	2760 ± 320
Line 3											
3–1	10.402225	99.195655	7.48	0.33	0.519	1.42	4.21	2.23	1.86 ± 0.18	5.7 ± 0.5	3880 ± 320
3–2	10.402413	99.198606	7.22	0.25	0.395	1.99	6.87	3.90	1.93 ± 0.19	5.6 ± 0.6	2920 ± 350
3–3	10.406903	99.205451	6.36	0.40	0.329	2.13	10.5	5.38	2.10 ± 0.20	5.8 ± 0.3	2790 ± 230
3–4	10.406086	99.210814	5.92	0.44	0.383	1.29	4.75	4.46	1.58 ± 0.15	5.4 ± 0.7	3410 ± 520
3–5	10.407722	99.211984	5.38	0.55	0.663	1.68	6.35	3.07	2.39 ± 0.23	5.6 ± 0.7	2360 ± 300
3–6	10.407356	99.219119	5.23	0.35	0.313	1.02	3.65	2.90	1.28 ± 0.12	3.1 ± 0.4	2440 ± 390
3–7	10.410536	99.223762	4.42	0.50	0.308	1.46	6.68	5.33	1.61 ± 0.16	2.7 ± 0.4	1680 ± 250

$Dist_s$: distance to the shore. D_e: total absorbed radiation dose.

outer ridge series gave the youngest age of deposition which ranges from 2790 ± 230–2760 ± 320 years ago.

At transect 3, three samples from the middle beach ridge display the depositional age ranging from 3880 ± 320–2790 ± 280 years BP. The outer beach ridge series with sand spit shape-like show a depositional age ranging from 3410 ± 520–1680 ± 250 years BP. Based on the result of age dating by OSL method, three series of the ancient beach ridges here show a depositional pattern seawards with the oldest one located at the inner beach ridge series and the youngest one located at the outer beach ridge series.

DISCUSSION

Palaeo-shoreline and palaeo-longshore currents

The delineation of palaeo-shorelines from aerial photograph interpretation is a pioneer technique used to locate the ancient shoreline in the central plain of Thailand[3,4]. The interpretation of aerial photographs alone however may not be reliable enough, and needs to be combined with a detailed analysis of sedimentology and dating of marine or brackish deposits as well as the classification of fauna found within the area.

In this study area, a tentative boundary of the westernmost palaeo-shoreline is indicated by the occurrence of an innermost beach ridge located far approximately 6 km inland from the present shoreline. However, the innermost beach ridge may have occurred either during the rapid transgression or regression; therefore, the back-barrier lagoon found in the west of innermost beach ridge (10 km inland) may help to confirm that the sea invasion occurred before the mid-Holocene.

Three sets of beach ridge plains were recognized in the study area as mentioned earlier. All the former beach ridges were prograded seawards. The orientation of the three beach ridge plains is parallel to the present shoreline and reflects a different direction of palaeo-longshore current during the time they were formed. The shape of the inner beaches shows that the deposition prograded northwards. They suggest that the longshore current direction was likely from south to north. On the other hand, the middle and the outer beaches show a spit shape with the end of each beach curved at the end; therefore, they were formed by the southwards direction of longshore current (also see Fig. 1c).

Sediment characteristics of the beach ridge

Differences in statistical parameters can be detected from each of beach ridge. Grain size distribution is one of the physical properties that reflect the energy during the depositional processes. However, grain size distribution could not be used alone for sedimentary environment identification, but it needs to be combined with the other lines of evidence (i.e., roundness, sphericity, and heavy minerals, biogenic components) [26].

Scatter plots of mean grain size versus standard deviation (sorting) shows a narrow range of grain size (very fine to coarse sand) and moderately to moderately well sorted values (also see Fig. 2). This indicates a high energy environment of the beach zone [23]. Based on the plot of sorting versus skewness, some samples from the outer and the inner beaches showed an extreme kurtosis and were well sorted indicating a neritic origin. The result of skewness versus kurtosis scatter plot reveals that half of all sediment samples are characterized by leptokurtic and are positively skewed. It indicates that the sediments were transported not so far from the source provenance [23]. Skewness and kurtosis plot is identified as the indicator of selective action of the transporting agent [27]. Additionally, all of sand generally yields a negative skewness that is common for a beach.

In this study, beach sand with fine- to coarse skewed indicates an environmental change between calm condition (stable current) and storm condition (variable current velocities and turbulence during deposition). Poorer sorting indicates variable current velocities and turbulence during deposition while good sorting indicated smooth and stable currents. Local shoaling in a shallow marine environment may produce a complex current flow patterns, eddying, and wave-generated turbulence causing sand to become negatively skewed for the most part [28].

Major beach sand composition is quartz. The rest are feldspar and ferromagnesian minerals. They are generally subangular to angular that can be classified as submature texture stage as suggested by Folk [29] and pointed to relatively short transportation for a considerable time and distance [30].

Pleistocene sea level records

Fleming et al [31] mentioned the eustatic component of relative sea-level change in Pleistocene provides a measure of the amount of ice transferred between the continents and oceans during glacial cycles. This has been quantified for the period since the last glacial maximum (LGM) by correcting observed sea-level change for the glacio-hydro-isostatic contributions using realistic ice distribution and earth models. During the LGM the eustatic sea level was at 125 ± 5 m lower than the present day [32].

In Southeast Asia, Hanebuth et al [9] proposed a sea-level curve for the Sunda shelf derived from shoreline facies. On the proximal part of the Sunda shelf transect, the late-glacial transgression could be directly identified between a water depth of 70 and 126 m. Pedogenesis on the late Pleistocene land surface indicates a low sea-level still stand in the LGM at 22 ka. This surface is overlaid by transgressive coastal sediment and marine sands then cover the transgressive sediments after a hiatus [9]. Ages from *Rotalia* sp. from mud layer vary widely from 12.4 to 4.1 ka and indicate that shelf sediments were reworked and mixed up to recent times.

A sea level curve in the Pleistocene epoch from the Huon Peninsula, New Guinea analysed from coral terraces shown a mean eustatic sea level change [32]. During 12 Ma, the sea-level began to fall and show fluctuation. The sea-level was lowest than mean eustatic sea level at 120 m below present mean sea level. Likewise, we infer that sea level records during LGM from the Gulf of Thailand is linked to the history of the Sunda Shelf.

Holocene sea level records and revised sea level curve

History of sea-level change in Southeast Asia during the Holocene was shown as sea level curve in Fig. 6a [33]. The curves were compiled from the Holocene records in Malacca strait, Indonesia [34], Malay-Thai peninsula, and Sunda shelf [9], and the Huon peninsula, Papua New Guinea from Chappell and Polach [35]. However, we will discuss only the previous work regarding Thai-Malay peninsula. Tjia [12] studied abrasion platforms, sea-level notches and oyster beds in peninsular Malaysia. The sea-level curve revealed the two Holocene highstands at 5000 and 2800 ^{14}C years BP [33]. However, sea-level in Thailand is mentioned to have fluctuated at least three times from mid/late Holocene highstands at 6000, 4000, and 2700 ^{14}C years BP [33]. Intertidal reef-flat corals (microatolls) formed in

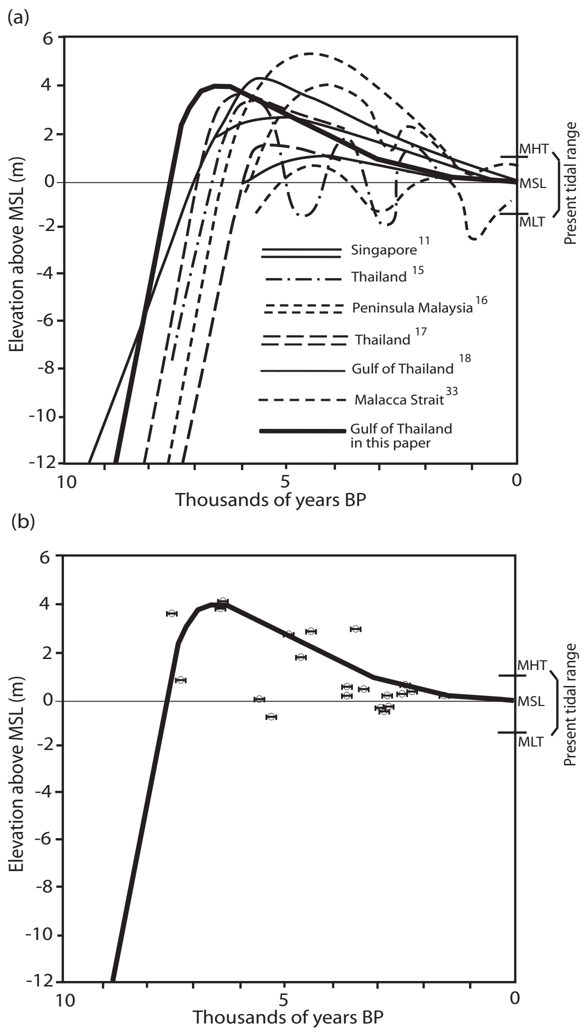

Fig. 6 (a) Sea-level curves from southeast Asia[33]. (b) A new revised sea level curve for Thailand proposed in this paper. Circles with horizontal lines represent the plots of age dating from OSL.

mid/late Holocene highstands were reported from Phuket, Southern Thailand[14]. The evidence there suggested a single Holocene highstand with a constant rate of sea level fall since 6000 years BP. The first sea-level curve for Thailand was proposed by Sinsakul et al[16]. The curve shows two Holocene highstands at 5000 and 2800 years BP[16]. In general, the sea-level curve for Thailand and Malaysia indicated three probable rebound phases during the mid- to Late Holocene with highstands at 6, 4, and 2.7 ka[12,16]. A revised sea-level envelope for the Gulf of Thailand was proposed by Choowong et al[17], which corresponded well with the sea-level curves subsequently constructed by Horton et al[18] for the Thai-Malay peninsula. The curves show an upward trend of rising Holocene sea level to the mid-Holocene highstand, and then a gradual fall of sea level to the present.

The interpretation of the former sea level has been commonly based on the coastal geomorphology, fossils, and absolute age dating. Here, we have done OSL dating of former beach ridge plains. We propose a revised sea level curve for Thailand (Fig. 6b). Together with the other geological evidence such as the occurrence of sea notches in different level and bio-erosion found at the wall of limestone, they all help to confirm that Chumphon estuary area was invaded by the sea during the Holocene. Sea level has reached almost 5 m above the present sea level. The alignment of the innermost beach ridges at highest elevation of 5 m indicates the highstand. Then the sea started to prograded seawards leading to the gradual formation of beach ridge plains at highstand elevation to the present MSL that can be inferred as marine regression (also see elevation change in Fig. 5e).

Acknowledgements: The 90th Anniversary of Chulalongkorn University Fund supported P.N. The Thailand Research Fund (BRG5780008) and Ratchadapiseksomphot Endowment Fund (RES560530028CC) provided funds to M.C. Thanks are also to EATGRU for OSL dating. Authors would like to express sincere acknowledge to editor-in-chief and anonymous reviewers that greatly improved the quality of manuscript.

REFERENCES

1. Takaya Y (1971) Two brackish clay beds along the Chao Phraya River of Thailand. *Tonan Ajia Kenkyu* **9**, 46–57.
2. Chonglakmani C, Ingavat R, Piccoli G, Robba E (1983) The last marine submersion of the Bangkok area in Thailand. *Mem Sci Geol* **36**, 343–52.
3. Supajanya T (1981) Delineation of the regression shorelines in the lower Chao Phraya Plain. In: *Proceedings of the Seventeenth Session, Committee for Coordination of Joint Prospecting for Mineral Resources*, pp 232–7.
4. Supajanya T (1983) Tentative correlation of old shorelines around the Gulf of Thailand. In: *First Symposium on Geomorphology and Quaternary Geology of Thailand*, Bangkok, Thailand, October 1983, pp 96–105.
5. Thiramongkol N (1983) Geomorphology of the lower central plain, Thailand. In: *Third Meeting of the Working Group on Geomorphology and Quaternary Geology of Thailand*, Bangkok, Thailand. October 1983, pp 13–25.

6. Somboon JRP, Thiramongkol N (1992) Holocene highstand shoreline of the Chao Phraya delta, Thailand. *J Southeast Asian Earth Sci* **7**, 53–60.
7. Sinsakul S (1992) Evidence of Quaternary sea level changes in the coastal areas of Thailand: a review. *J Southeast Asian Earth Sci* **7**, 23–37.
8. Intasen W, Tepsuwan T, Seritrakul S (1999) Seismic facies, stratigraphy and evolutionary model of the late Quaternary deposits in the Lower Central Plain of Thailand. In: *Proceeding on the Thai-Japanese Geological Meeting: Comprehensive Assessments on Impact of Sea-Level Rise*, November 30–December 4, 1999, Petchaburi, Thailand, pp 108–24.
9. Hanebuth T, Stattegger K, Grootes MP (2000) Rapid flooding of the Sunda shelf: A late-glacial sea-level record. *Science* **288**, 1033–5.
10. Woodroffe SA, Horton BP (2005) Holocene sea-level changes in the Indo-Pacific. *J Asian Earth Sci* **25**, 29–43.
11. Hesp PA, Hung CC, Hilton M, Ming CL, Turner IM (1998) A first tentative Holocene sea-level curve for Singapore. *J Coast Res* **14**, 308–14.
12. Tjia HD (1987) Change of sea level in the southern South China Sea area during Quaternary times. In: *Proceedings of Symposium on Quaternary Geology of the Malay-Indonesian Coastal and offshore Area (CCOP Report, CCOP/TP.5)*, pp 11–36.
13. Dheeradilok P (1995) Quaternary coastal morphology and deposition in Thailand. *Quaternary Int* **26**, 49–54.
14. Scoffin TP, Le Tissier MDA (1998) Late Holocene sea level and reef-flat progradation, Phuket, South Thailand. *Coral Reefs* **17**, 273–6.
15. Choowong M (2002) The geomorphology and assessment of indicators of sea-level change to study coastal evolution from the gulf of Thailand. In: *International Symposium on "Geology of Thailand" Department of Mineral Resource*, Bangkok Thailand, August, 2002, pp 207–20.
16. Sinsakul S, Sonsuk M, Hasting PJ (1985) Holocene sea levels in Thailand: evidence and basis for interpretation. *J Geol Soc Thai* **8**, 1–12.
17. Choowong M, Ugai H, Charoentitirat T, Charusiri P, Daorerk V, Songmuang R, Ladachart R (2004) Holocene biostratigraphical records in coastal deposit from Sam Roi Yod National Park, Prachuap Khiri Khan, Western Thailand. *Nat Hist J Chula Univ* **4**, 1–18.
18. Horton BP, Gibbard PL, Milne GM, Morley RJ, Purintavaragul C, Stargardt JM (2005) Holocene sea levels and paleoenvironments, Malay-Thai Peninsula, southeast Asia. *Holocene* **15**, 1199–213.
19. Boggs S Jr (1987) *Principles of Sedimentology and Stratigraphy*. Merrill Publishing Co., Ltd, Columbus, Ohio.
20. Blott SJ, Pye K (2001) GRADISTAT: A grain size distribution and statistics package for the analysis of unconsolidated sediments. *Earth Surf Process Landf* **26**, 1237–48.
21. Compton RR (1962) *Manual of Field Geology*. Wiley. New York. pp 36–47.
22. Powers MC (1953) A new roundness scale for sedimentary particles. *J Sediment Petrol* **23**, 117–9.
23. Folk RL, Ward WC (1957) Brazos River bar [Texas]; a study in the significance of grain size parameters. *J Sediment Res* **27**, 3–26.
24. Larson R, Morang A, Gorman L (1997) Monitoring the coastal environment; Part II: Sediment sampling and geotechnical methods. *J Coast Res* **13**, 308–30.
25. Thongpinyochai A (1996) *Geology of Chumphon Province in Minerals Resources Regional Office 2 (Phuket) Report*. Department of Mineral Resource, Ministry of Industry, Thailand.
26. Martins LR, Barboza EG (2005) Sand-gravel marine deposits and grain-size properties. *Gravel* **3**, 59–70.
27. Martins LR (1965) Significance of skewness and kurtosis in environmental interpretation. *J Sediment Res* **35**, 768–70.
28. Amaral EJ, Pryor WA (1997) Depositional environment of the St. Peter Sandstone deduced by textural analysis. *J Sediment Res* **47**, 32–52.
29. Folk RL (1951) Stage of textural maturity in sedimentary rock. *J Sediment Res* **21**, 127–30.
30. Friedman GM (1967) Dynamic processes and statistical parameters compared for size frequency distribution of beach and river sands. *J Sediment Res* **37**, 327–54.
31. Fleming K, Johnston P, Zwartz D, Yokoyama Y, Lambeck K, Chappell J (1998) Refining the eustatic sea-level curve since the Last Glacial Maximum using far- and intermediate-field sites. *Earth Planet Sci Lett* **163**, 327–42.
32. Pillans B, Chappell J, Naish TR (1998) A review of the Milankovitch climatic beat: template for Plio–Pleistocene sea-level changes and sequence stratigraphy. *Sediment Geol* **122**, 5–21.
33. Choowong M (2011) Quaternary. In: Ridd MF, Barber AJ, Crow MJ (eds) *Geology of Thailand* (Chapter 12). Geological Society of London, pp 335–50.
34. Geyh MA, Streif H, Kudrass HR (1979) Sea-level changes during the late Pleistocene and Holocene in the Strait of Malacca. *Nature* **278**, 441–3.
35. Chappell J, Polach H (1991) Post-glacial sea-level rise from a coral record at Huon Peninsula, Papua New Guinea. *Nature* **349**, 147–9.